**Article:**
Hutchinson, A.J. and Gladwin, D.T. (2022) Techno-economic assessment of novel hybrid energy storage control strategies for dynamic frequency response. Journal of Energy Storage, 55, Part D. 105694. ISSN: 2352-152X

https://doi.org/10.1016/j.est.2022.105694

Journal of Energy Storage 55 (2022) 105694

Contents lists available at ScienceDirect

Journal of Energy Storage

journal homepage: www.elsevier.com/locate/est

Research papers

# Techno-economic assessment of novel hybrid energy storage control strategies for Dynamic Frequency Response☆

Andrew J. Hutchinson *,[1], Daniel T. Gladwin[2]

*University of Sheffield, Western Bank, Sheffield, S10 2TN, United Kingdom*

ARTICLE INFO

*Keywords:*
Energy storage
Flywheels
Frequency response
Control strategies
Hybrid

ABSTRACT

Frequency Response services are a key part of the operation of the Great Britain (GB) Electricity Grid system. One of the most prevalent areas for energy storage deployment is in providing dynamic frequency response services. Battery Energy Storage Systems (BESSs) are the most deployed storage medium for this application, but are vulnerable to high cycle rates and degradation. Flywheel Energy Storage Systems (FESSs) are far more resilient to cycle based degradation and by co-locating them with a BESS they can extend the life of the battery cells and improve the overall Net Present Value (NPV) of the system. This paper presents for the first time a detailed techno-economic analysis of 7 novel control strategies for hybrid systems and performs an in depth techno-economic analysis on the 3 strategies that show the most potential for real world deployment. Crucially, it produces novel and wide ranging results on the utilisation of FESSs for this application, giving a clear and detailed account of the price that flywheel manufacturers will need to achieve for their products to be viable in this field for the first time. It is demonstrated how these novel control strategies can be designed and refined to maximise the technical performance with a subsequent techno-economic analysis conducted to assess the most promising control strategies effectiveness, and a novel investigation carried out into the minimum total capital cost (TCC) that a FESS needs be priced at to achieve to a positive NPV change under these control strategies. Under general conditions, the threshold TCC below which a positive NPV change is achieved is between £550/kW and £5,855/kW for the various control strategies and FESS configurations, showing that a wide range of different FESSs can be economically viable under the correct control strategy.

## 1. Introduction

Deployment of energy storage systems (ESSs) has been increasing rapidly in line with the changing landscape of energy generation and distribution with a move towards intermittent renewable generation and electric transportation. In Great Britain (GB), Dynamic Frequency Response (DFR) is a mechanism that National Grid ESO utilises to maintain the grid frequency at 50 Hz. Contracted installations of energy storage respond to fluctuations in frequency in response to a set response envelope [1].

This paper focuses on the system level frequency control over extended periods of time as intended by the DFR service, rather than transient frequency events or microgrid interactions as detailed elsewhere in literature [2,3].

With the launch of several new frequency response services, Dynamic Containment (DC), Dynamic Regulation (DR) and Dynamic Moderation (DM) [4], there will be increasing opportunities for ESSs to be deployed in this field. Due to it operating over a significant amount of time, DFR represents an excellent starting point for assessing the validity of proposed ESSs with operational and financial information widely available [5,6].

The response envelope employed by DFR is shown in Fig. 1. Frequency response services across the world have been the subject of many studies relating to energy storage, generation and distribution in micro grids [7–11].

The most commonly deployed energy storage medium for these applications are Battery Energy Storage Systems (BESSs). They are a mature technology that generally has a large energy capacity [12], enabling them to provide services for longer periods of time compared

☆ The authors gratefully acknowledge the financial support of the Engineering and Physical Sciences Research Council (EPSRC) in the form of the 'Energy Storage and its Applications' Centre for Doctoral Training under grant code EP/L0168/18.

* Corresponding author.
*E-mail address:* ahutchinson1@sheffield.ac.uk (A.J. Hutchinson).
[1] Researcher
[2] Supervisor

https://doi.org/10.1016/j.est.2022.105694
Received 12 July 2022; Received in revised form 25 August 2022; Accepted 16 September 2022
Available online 30 September 2022

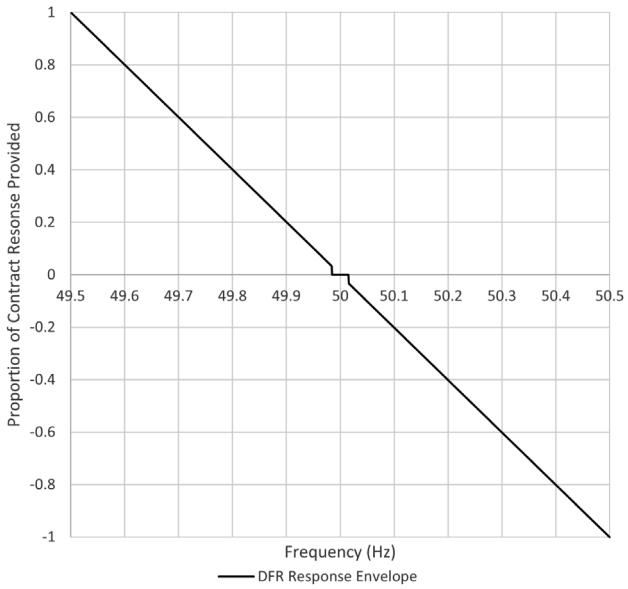


**Fig. 1.** DFR response envelope.

to shorter duration energy storage such as Flywheel Energy Storage Systems (FESSs).

However, BESSs are generally far more susceptible to cycle based degradation [13,14] which for some applications leads to shorter lifespans and hence lower economic return. FESSs on the other hand are far more resilient to cycle based degradation but lack the energy capacity to perform these services on their own [15]. An opportunity therefore exists to hybridise the two technologies and exploit the strengths of both systems to mitigate weaknesses.

Whilst BESSs are now relatively commercially mature, FESSs are yet to achieve a similar status. It is therefore imperative that as these commercial systems are being developed that studies are undertaken to guide the industry towards both the correct applications and the correct product cost targets. This is the primary motivation of this study, to present novel scenarios for the implementation of FESSs and reveal the required economic characteristics for them to be successful.

### 1.1. Literature review

Hybrid Energy Storage Systems (HESSs) are commonly studied in the literature for a wide range of applications from oil drilling rigs [16] to renewable generation systems [17]. BESSs are prevalent throughout the literature as the 'energy' portion of the proposed hybrid systems whilst the 'power' portion of the hybrid system is often provided by flywheels or super capacitors.

In [18] the author presents a system that compensates for power fluctuation where the energy component is a BESS and the power component is a FESS, showing better performance when using a hybrid system compared to BESS alone however it lacks a financial analysis to provide a real world context to how viable the system is.

In terms of degradation mitigation, a main driver for attempting hybridisation of different energy stores, [19] shows that by using a hybrid system a BESS lifetime can be extended from 5.7 years to 9.2 years in the context of a frequency control system for a microgrid. This is not the only study to cite lifetime improvements to a BESS through the introduction of a FESS, with the work in [20] showcasing a maximum improvement of 3.6 years when hybridising lithium ion batteries with a flywheel for a solar generation site.

Additionally, [21] shows how a control system can be organised to expose a Flywheel to the higher frequency components whilst the Battery delivers on lower frequency events within a rail application to good effect. [22] shows that a BESS that performs technically well will not always be suitable for deployment, as the study shows that any benefit that the BESS creates in this scenario is outweighed by the increased capital costs and decrease to the overall renewable plant efficiency.

A vital part of any HESS is the control mechanism, determining when and how each separate medium is utilised in order to maximise the effectiveness of the HESS. The control system chosen can have a significant effect on both the operational performance, and the sizes of the optimal configurations of the individual systems. Many pieces of work have assessed the effectiveness of different control mechanisms on ESSs [19,23–25].

One of the most pertinent pieces of work already conducted in this field is [26] which assesses the effect of introducing a FESS to operate alongside a BESS providing a frequency response service and subsequently the impact on degradation that results from this hybridisation. The control strategy implemented consists of a low pass filter that separates the components of requested power, the FESS delivering high frequency components and the BESS delivering low frequency components.

It is a promising study that lays good foundations for further works with several areas that could be developed further, such as length of simulation, varying FESS size, economic analysis and differing control strategies. The work presented in this paper aims to expand upon this work with detailed sensitivity and economic analysis and propose further novel control strategies to increase the benefit to the overall system

Another study also looks at hybrid FESS/BESS for frequency based services in Germany [27]. This study also shows promising results with a reduction in battery degradation achieved through the introduction of a flywheel. Again, the analysis performed is a robust experimental study that lays good foundation for further works to explore more complex control systems operating over longer periods of time as well as a more detailed economical study that can only efficiently be achieved through modelling and simulation works. This paper again builds upon the previous works to take real world data and use rapid simulations to produce a wide range of different analysis. It will also consider the key metric of availability over the operational period which is not considered in either [26] or [27] and is vital to understanding the viability of a service operating over months or years.

### 1.2. Novel contribution

In this paper, a novel suite of high level control strategies for Hybrid Energy Storage Systems delivering continuous DFR are presented. These control strategies offer new and important ways of maximising the impact that introducing alternative energy storage systems to a battery energy storage system. The study is backed up by both a novel in depth technical assessment of the performance and settings of each control strategy as well as a novel and wide ranging economic study.

Crucially, this study shows for the first time the required Total Capital Cost (TCC) that a FESS is required to achieve in order to provide a positive economic impact, giving key insight to industrial developers of the technology.

The main contributions are summarised as follows;

- Introduction of a FESS into a BESS providing a DFR service
- Development of novel control strategies for maximising performance of the site in relation to the baseline BESS-Only case
- Degradation modelling for the BESS under varying configurations and control strategies
- Refinement and sensitivity analysis of control strategy settings
- Extensive economic analysis showing required costs for a FESS to be viable in this application

**Table 1**
Description of each control strategy to be assessed.

| Control strategy Designation | Description |
|---|---|
| 1 | A 1 MW/1 MWh battery used as a baseline to compare with the remaining control strategies. The BESS delivers the required DFR power for all requests whilst it remains within SOC limits. No FESS is included. |
| 2 | The FESS acts as a filter to the BESS, responding to any request that it is available to meet. Only if the FESS cannot meet the power requirements is the request passed on to the BESS. |
| 3 | The FESS takes on any requests outside of a designated frequency range, with the BESS responding to any requests inside the range. For example, a FESS could meet any requests below 49.9 Hz and above 50.1 Hz, whilst the BESS meets any requests in the 49.9–50.1 Hz range. |
| 4 | The FESS takes on any requests inside of a designated frequency range, with the BESS responding to any requests outside the range. For example, a BESS could meet any requests below 49.9 Hz and above 50.1 Hz, whilst the FESS meets any requests in the 49.9–50.1 Hz range. |
| 5 | Any power request is split between the two systems according to the ratio of the FESS maximum power output to the agreed service. For example, a 1 MW service and a 0.2 MW FESS would have each power demand split at a ratio of 5:1 between BESS and FESS. |
| 6 | The FESS provides the 30-s rolling average of the requested power, with the BESS making up any difference between the power delivered by the FESS and the instantaneous request. |
| 7 | The BESS provides the 30-s rolling average of the requested power, with the FESS making up any difference between the power delivered by the BESS and the instantaneous request. |
| 8 | The responsibility for providing the service alternates between the two systems over a set period. For example, a FESS will deliver the service for 30-mins followed by the BESS delivering for the next 30-mins. |

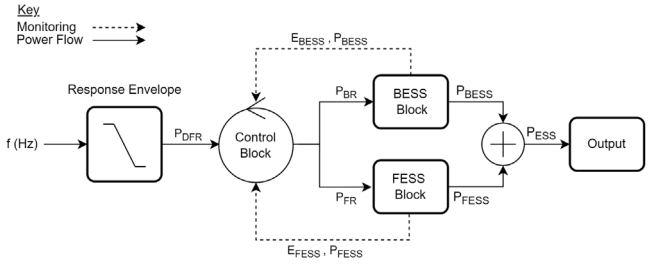


**Fig. 2.** High level diagram of basic simulation operation.

## 2. Study overview

This study is being carried out in MATLAB/Simulink using a FESS and BESS model developed over numerous years and discussed previously in [14,28]. This configuration of the BESS model has been taken from a statistically verified analysis of a BESS owned and operated by The University of Sheffield [29,30] whilst the FESS model has been developed from manufacturer provided data and characteristics. The simulation is conducted using frequency data from October 2020 to September 2021 and payment is based upon the average availability payment tendered during the same time period [5].

Fig. 2 shows a high level diagram of the model utilised for this work where $P_{DFR}$ is the power requested by the service in kW, $P_{BR}$ and $P_{FR}$ are the power request (kW) to the BESS and FESS respectively, $E_{BESS}$ and $E_{FESS}$ are the instantaneous energy available (kWh) within the BESS and FESS respectively, $P_{BESS}$ and $P_{FESS}$ are the instantaneous power output (kW) from the BESS and FESS respectively, and $P_{ESS}$ is the instantaneous power output (kW) of the HESS as a whole.

Eight different control strategies have been assessed within this piece of work, consisting of a BESS only baseline and 7 hybrid control strategies. Table 1 contains a brief description of each control strategy, with control diagrams contained within later sections wherever the control strategy has been explored in further detail. The baseline which each control strategy is to be measured against consists of a 1 MW/1 MWh BESS delivering a 24/7 1 MW service. Using this approach it can be shown how the key metrics such as availability, Net Present Value and BESS degradation change according to hybrid configuration and control mechanism.

The control strategies were refined over the course of multiple case studies and bodies of work. They were developed by identifying areas of the hybrid system that could be varied, and performing an iterative design process to test the effects. As part of this process, some control strategies were already dismissed due to poor performance or unrealistic implementation opportunities, leaving the 7 control strategies discussed in this paper. Similar control schemes have been found within literature, such as in [26] which presents a similar control scheme to CS-3 and CS-4.

$$A_{vail}(\%) = \frac{\sum_{t=0}^{t_{end}} x}{t_{end}} \begin{cases} x = 1 & P_{ESS} = P_{DFR} \\ x = 0 & otherwise \end{cases} \quad (1)$$

The key technical and financial parameters that have been used in this study are shown in Table 2. The main criteria that each control strategy will be assessed on is as follows;

- Availability — Availability can be expressed as shown in Eq. (1) where $t_{end}$ is simulation time end in seconds, $P_{DFR}$ is the requested power from the response envelope and $P_{ESS}$ is the power provided by the ESS. If $P_{ESS}$ is equal to $P_{DFR}$ the service is deemed available for that 1 s period and if not it is deemed unavailable. The total availability is the sum of all available seconds as a proportion of total simulated seconds. Broadly, it is defined as the total amount of time that the ESS is able to meet the required power demands as a percentage of the overall operational time. It is this metric that is used to determine the payment provided for the service, with no payment proved below 90% followed by a sliding scale from 90%–95% where it reaches full payment. The availability payment has been set as £11.67/MW/hr in line with the average payment provided over the previous 12 months [5]. A system would become unavailable due to reaching high or low State of Charge (SOC) limits i.e. having no stored energy left to provide a requested discharge.
- BESS Degradation — The overall reduction in battery capacity expressed as a percentage of the original capacity. For instance, a 1MWh BESS suffering 5% degradation would have 0.95MWh of capacity. Within this study, a degradation algorithm has been implemented within MATLAB/Simulink based upon the work conducted in [31,32] which assigns a percentage degradation based upon instantaneous C-Rate and energy throughput.
- FESS Total Capital Cost (TCC) - The cost in £/kW required to install the specific FESS configuration. This will be assessed to determine the maximum TCC at which a FESS can create a positive NPVC in the hybrid system, showing that any TCC below this value results in increased positive NPVC. For instance, if a FESS configuration had a threshold cost of £1000/kW it would mean that any TCC below this would generate increased positive NPVC.

**Table 2**
Parameters used in the simulation.

| Parameter | Value | Parameter | Value |
|---|---|---|---|
| BESS capacity | 1 MWh | BESS C-Rate | 1 |
| Availability fee (£/MW/hr) | 11.7 | BESS TCC (kW) | £468/kW |
| BESS cycle limit | 10000 | FESS cycle limit | 100000 |
| Discount rate | 5% | Payback period | 25 years |
| Start month | Nov 2020 | End month | Oct 2021 |

- Net Present Value Change (NPVC) - From a normalised baseline of a 1MWh/1MW BESS providing a 1MW service, how does the overall NPV of the system increase or decrease under various control strategies and hybrid configurations. Net Present Value is given in the industry standard Eq. (2) and seeks to place a value on a given investment taking into account initial capital costs and future costs and revenue. In Eq. (2), $N$ is the total operational lifetime, $C_{capital}$ is the capital expenditure over the lifetime of the system, $C_{revenue}$ is the yearly revenue of the installation, and d is the discount rate as a %, representing the rate of return required.

$$NPV = \sum_{n-1}^{N} \frac{C_{revenue}}{(1+d)^n} - C_{capital} \quad (2)$$

## 3. Initial assessment

As a starting point, the values for FESS energy capacity and C-Rate determined by a previously published genetic algorithm study concentrating on CS-2 and CS-6 were used for all 7 hybrid control strategies [33]. The sizing determined by this work consisted of a 60 kWh 4C FESS and was shown to be the optimum solution for providing a positive NPVC to the hybrid system. The results of a year long simulation using these specifications for each control strategy are shown in Table 3.

This initial set of simulations can be used to identify which control strategies are viable to investigate further and refine to their specific strengths. The baseline to which all subsequent control strategies will be compared is CS-1 (BESS Only) where it can be seen that the average availability is 96.33% and a high overall degradation over the course of 1 year is 13.15% due to the high cycle count (1304 over 1 year).

This is a prohibitive amount of degradation for the service to be viable as the system would need replacing every 7.6 years, and so this is one of the key areas that will be assessed with the remaining control systems. CS-2 and CS-6 have been optimised and discussed in a conference paper awaiting publication and hence will not be further explored within this paper. A genetic algorithm was used to determine the optimum size and C-Rate of the FESS forming part of the hybrid system with the goal of maximising positive NPVC. The outcome of both optimisations was a 60 kWh 4C FESS.

CS4, where the FESS takes control of all requests within a set frequency band and the BESS takes control of all requests outside of that band, shows the lowest amount of BESS degradation over the course of a year, decreasing from 13.15% when a BESS is operating alone to 2.65% under this control strategy. However it also has a very low availability, which will result in a poor economic performance. This control strategy is therefore worth investigating further to determine whether it can be modified to provide a stronger overall performance.

Alternatively CS-3 and CS-7 represent the lowest amount of degradation reduction for the BESS with values of 9.84% and 12.40% respectively over the course of a year. Considering that neither of these control strategies offer greater availability than other control strategies studied that provide a much greater degradation reduction, these will not be progressed any further.

CS-5 shows excellent availability and a moderately reduced level of BESS degradation. However, the lack of FESS cycles present in this control strategy suggests that it could be utilised in a more significant role to reduce the degradation further. This will be investigated further to determine if changing the FESS size can provide a more balanced solution.

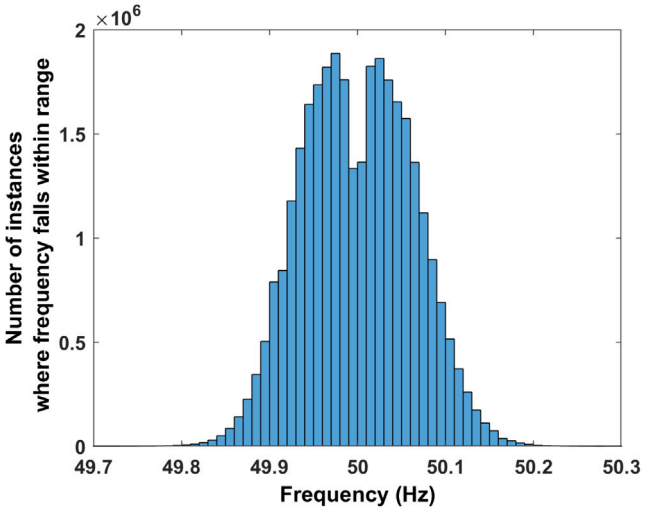


**Fig. 3.** Histogram showing the number of instances the grid frequency falls within given ranges (a bin width of 0.01) over the course of a year between November 2020 and October 2021.

Finally, CS-8 also represents a potentially exploitable initial assessment, offering reduced BESS degradation with a low average availability. This control strategy can be further investigated to assess whether the availability can be increased by modifying either the duration for the alternating energy storage operations, or by evaluating different configurations of FESS.

## 4. Control strategy 4

As discussed in Table 1, this control strategy operates by assigning all of the power request derived from a frequency within a set threshold to the FESS, and anything outside of this threshold to the BESS. For the initial assessment of this control strategy, the thresholds have been set as 49.9 Hz for the lower band limit and 50.1 Hz for the upper band limit, meaning any frequency response in the 49.9–50.1 Hz range will be delivered by the FESS and anything outside will be delivered by the BESS.

As can be seen from Fig. 3 which shows a histogram of the frequency over the period November 2020–October 2021, this would cover a vast amount of the time in which the service would be expected to operate, with the majority of the frequency instances falling within this 49.9 Hz–50.1 Hz range and minimal activity outside of it.

Fig. 4 shows the flowchart for how this strategy is executed, where $f_{Low}$ is the lower frequency threshold, $f_{High}$ is the high frequency threshold, $P_{DFR}$ is the required power requested by the response envelope and $P_{BESS}$ and $P_{FESS}$ are the power output from the BESS and FESS respectively. $P_{FAvail}$ and $P_{BAvail}$ represent the maximum power available to each ESS when they cannot meet the full requested power. Fig. 5 shows the model in operation for this control strategy.

### 4.1. Energy capacity sensitivity

The first step to assessing how the performance of this control strategy can be improved is to determine the performance over a wide range of different FESS configurations. The simulation was therefore executed over a range of 100 kWh to 1 MWh FESS maintaining the C-Rate at 4C. Note that for this control strategy, an initial study on

**Table 3**
Initial results of control strategy analysis.

| | CS-1 | CS-2 | CS-3 | CS-4 | CS-5 | CS-6 | CS-7 | CS-8 |
|---|---|---|---|---|---|---|---|---|
| Availability (%) | 96.33% | 95.83% | 94.25% | 86.40% | 96.95% | 96.93% | 96.77% | 90.00% |
| BESS cycles | 1304 | 525 | 986 | 305 | 986 | 609 | 1297 | 638 |
| FESS cycles | 0.0 | 7998 | 1872 | 7165 | 2730 | 7995 | 1513 | 4516 |
| BESS degradation (%) | 13.15% | 5.05% | 9.84% | 2.65% | 9.92% | 5.93% | 12.40% | 6.13% |
| Approx years till replacement | 7.6 | 19.8 | 10.2 | 25.0 | 10.1 | 16.9 | 8.1 | 16.3 |

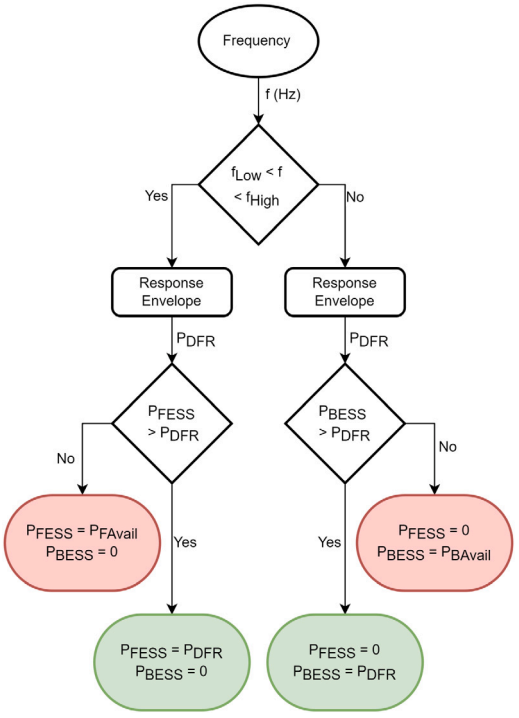


**Fig. 4.** Control diagram and flowchart for Control strategy 4.

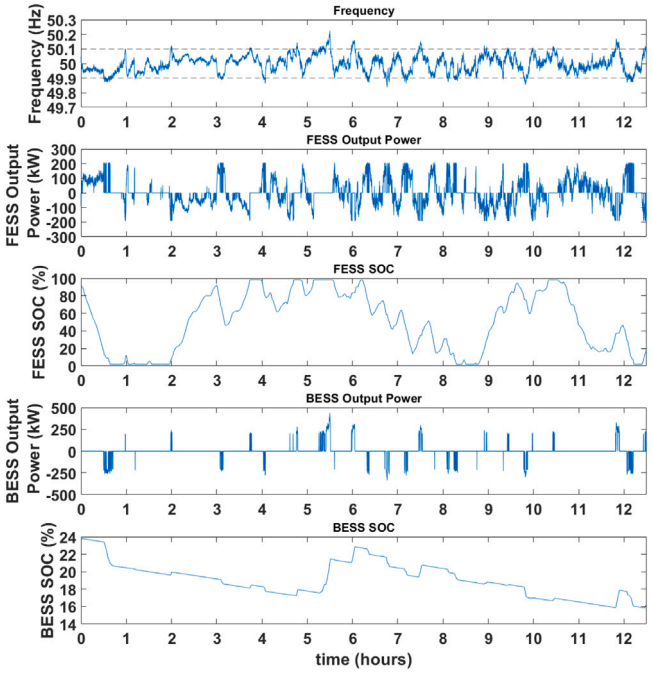


**Fig. 5.** Simulation outputs when operating a 1MW 1C BESS with a 60 kW 4C FESS under CS-4.

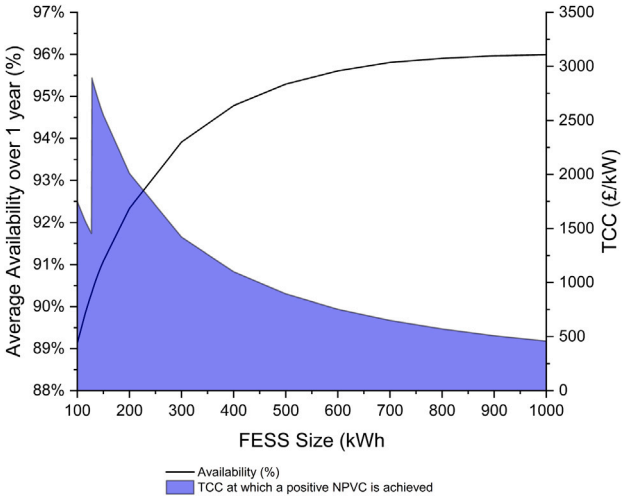


**Fig. 6.** Average availability and threshold cost for FESS to provide a positive NPVC across varying FESS sizes for CS-4. The shaded area represents values of TCC where a positive NPVC would be achieved.

**Table 4**
Excerpt of NPVC results from frequency threshold variation for CS-4, rounded to the nearest £k.

| NPVC (£k) | | Lower frequency threshold (Hz) | | |
|---|---|---|---|---|
| | | 49.92 | 49.91 | 49.9 |
| Upper frequency threshold (Hz) | 50.08 | −£34 | −£343 | −£404 |
| | 50.09 | −£17 | £45 | £54 |
| | 50.1 | −£137 | −£46 | £0 |

varying C-Rates was carried out and shown that increasing the C-Rate did not provide any performance benefit and purely resulted in increased costs and therefore decreased economic value.

The results of varying the FESS energy capacity are shown in Fig. 6 where both average availability and the threshold TCC for a positive NPVC is displayed. Clearly as the energy capacity of the system is increased the availability increases in line with this, plateauing at 96% availability. Conversely, as the energy capacity is decreased the threshold for positive NPVC increases to a peak of £2893/kW before dropping back down again.

This sheer drop occurs as the system reaches a point of generating significantly less income due to low availability. It subsequently rises again when decreasing beyond this point as there is minimal further reduction in income but continuous reduction in TCC as the FESS gets smaller.

### 4.2. Control strategy settings sensitivity

Taking the results from the previous section into account, the simulation was then run with varying settings for the high and low frequency boundaries, taking into account the histogram shown in Fig. 3 and noting that as the frequency range for FESS operation is reduced, the BESS will be asked to operate with increasing regularity,

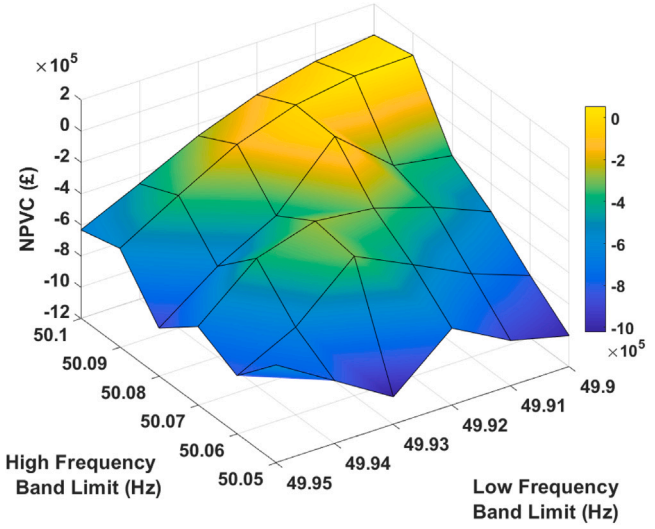


**Fig. 7.** NPVC for varying high and low frequency threshold set points for CS-4.

**Table 5**
Excerpt of BESS degradation results from frequency threshold variation for CS-4.

| BESS degradation | | Lower frequency threshold (Hz) | | |
|---|---|---|---|---|
| | | 49.92 | 49.91 | 49.9 |
| Upper frequency threshold (Hz) | 50.08 | 5.0% | 4.9% | 4.5% |
| | 50.09 | 3.8% | 3.7% | 3.6% |
| | 50.1 | 2.8% | 2.7% | 2.6% |

**Table 6**
Excerpt of average availability results from frequency threshold variation for CS-4.

| Average availability | | Lower frequency threshold (Hz) | | |
|---|---|---|---|---|
| | | 49.92 | 49.91 | 49.9 |
| Upper frequency threshold (Hz) | 50.08 | 92.6% | 92.4% | 91.4% |
| | 50.09 | 91.1% | 91.4% | 91.3% |
| | 50.1 | 89.5% | 90.2% | 90.3% |

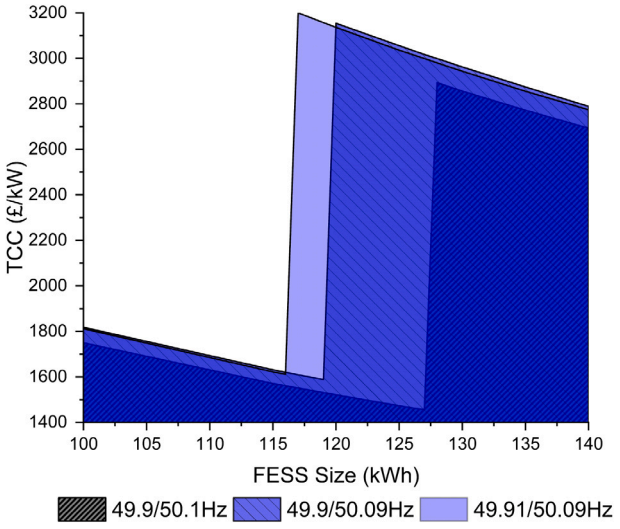


**Fig. 8.** Threshold TCC for a FESS to provide a positive NPVC at varying energy capacities for CS-4.

with a steep increase in operating time as the frequency gets closer to 50 Hz.

The low boundary was varied between 49.9 Hz and 49.95 Hz in 0.1 Hz intervals, and the high boundary was varied between 50.05 Hz and 50.1 Hz also in 0.1 Hz intervals. The resulting NPVC was then plotted for each combination of high and low frequency boundaries, as seen in Fig. 7 with Tables 4 showing the values for the upper region of the graph.

For the majority of alternate set points the NPVC is greatly reduced. However, for the 49.9/50.09 Hz and the 49.91/50.09 Hz combination the NPVC is greater than the original 49.9/50.1 Hz combination. This asymmetry takes advantage of sacrificing a small amount of BESS degradation for an increase in average availability. These results suggest that further improvements can be made by re-performing the energy capacity sensitivity analysis conducted previously with the two new pairs of set points.

In Table 5, which details the level of degradation the BESS experiences under each combination of settings, it can be seen that a significant reduction in overall BESS degradation can be achieved for all combinations, but with the most significant reductions being achieved when the Upper Frequency Threshold is set at 50.1 Hz as this is when the BESS will be operating the least. Where lower levels of degradation are present this would lead to an extended BESS lifetime and subsequent improvements to the economic performance of the site.

In Table 6, which details the average availability under each combination of settings, it can be seen that there is not significant variation between all of the combinations. Whilst the availability peaks at 92.6% with the 50.08/49.92 Hz combination, this only drops by 3.1% when considering the worst combination (50.1/49.92 Hz). Whilst the availability has been improved from the initial assessment, it still does not reach the ideal level of 95% average availability which is a significant drawback of the strategy.

### 4.3. Re-assessing energy capacity

The previous energy capacity sensitivity analysis was repeated this time using firstly a 49.9/50.09 Hz and secondly a 49.91/50.09 Hz set point combination. Fig. 8 shows a focused view of Fig. 6, displaying the 100–140 kWh region of the results where the peak for all three studied frequency combinations occurs.

For the 49.9/50.09 Hz combination, the FESS size with the highest possible TCC to provide positive NPVC occurs at 120 kWh compared to the previously determined 128 kWh for the 49.9/50.1 Hz combination, and additionally will now provide a positive NPVC up to a value of £3154/kW compared to a previous value of £2893/kW.

When using set points of 49.91/50.09 Hz the FESS size which provides the highest possible TCC for a positive NPVC is 117 kWh which can provide a positive NPV up to a value of £3200/kW. This indicates that the 49.91/50.09 Hz pairing represents the best settings for this control strategy.

For the two variations on set point combinations, the sudden fall in TCC for a positive NPVC occurs at a lower energy capacity than in the original set point combination. Changing the set points in this way transfers a small amount of the energy throughput from the FESS to the BESS, sacrificing a minimal increase in degradation for an increase in availability.

### 4.4. Current economic implications

A range of different literature places the TCC for a FESS in the range of £500–2500/kWh [12,34–36]. The simulation was executed using different TCC values throughout this range as well as using the control settings determined above and taking the optimal FESS configuration for the 49.91/50.09 Hz set point. The NPVC for a range of different TCC values was produced and plotted in Fig. 9.

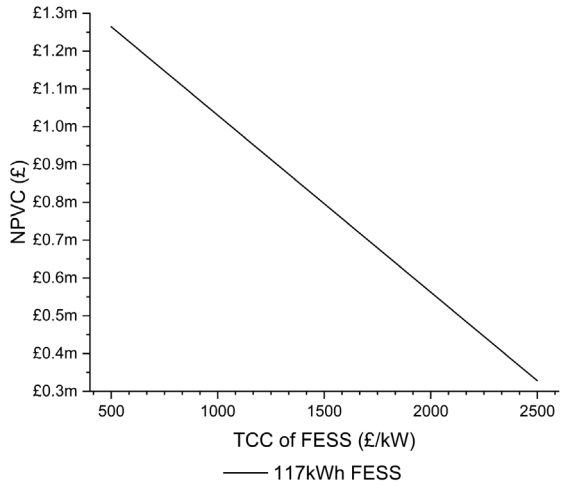


**Fig. 9.** NPVC when introducing a 117 kWh FESS of varying TCC for CS-4.

**Table 7**
Examples of ratio of demand split for varying levels of FESS rated power.

| Fess rated power (kW) | FESS contribution | BESS contribution |
|---|---|---|
| 200 | 20% | 80% |
| 300 | 30% | 70% |
| 500 | 50% | 50% |

The chart shows as expected that as the TCC increases the scale of positive NPVC is reduced with a linear relationship identified. Assuming a TCC at the lower end of the available literature, the hybridisation under this control strategy would increase the NPV of the system by £1.4 m. Even at the upper end of the available literature TCC, the NPV would be increased by £328,320, showing a strong case for the effectiveness of this control strategy (CS-4) despite the lower than ideal level of availability.

## 5. Control strategy 5

For this control strategy, the power demand is split according to the power rating of each HESS component. Under the initial simulation this control strategy achieved an average availability of 96.95% and a total BESS degradation of 9.92%. The are two main variables that will affect the effectiveness of this control strategy, the FESS energy capacity and the FESS C-Rate.

The initial set of simulations were performed with the following controls set to split the power request according to the ratio of 100% of the FESS Max Power to the overall service. Example ratios are shown in Table 7. Fig. 10 shows the flowchart for how this strategy is executed where $P_{BReq}$ and $P_{FReq}$ are the requested power from the BESS and FESS respectively.

### 5.1. C-Rate and energy capacity sensitivity analysis

Shown in Tables 8 and 9 are the performance results from varying the energy capacity between 15 kWh and 250 kWh and the C-Rate between 4 and 16C. Note that the greyed out sections of the tables represent hybrid combinations that are not relevant for this control strategy as the FESS contribution would render the BESS irrelevant and hence is an unrealistic scenario to consider.

The results show that there is a minimal impact on overall availability when the configuration of the FESS is varied, with the average availability ranging from 95.92% to 96.97% for the configurations tested. On the other hand, there is a significant impact on the BESS

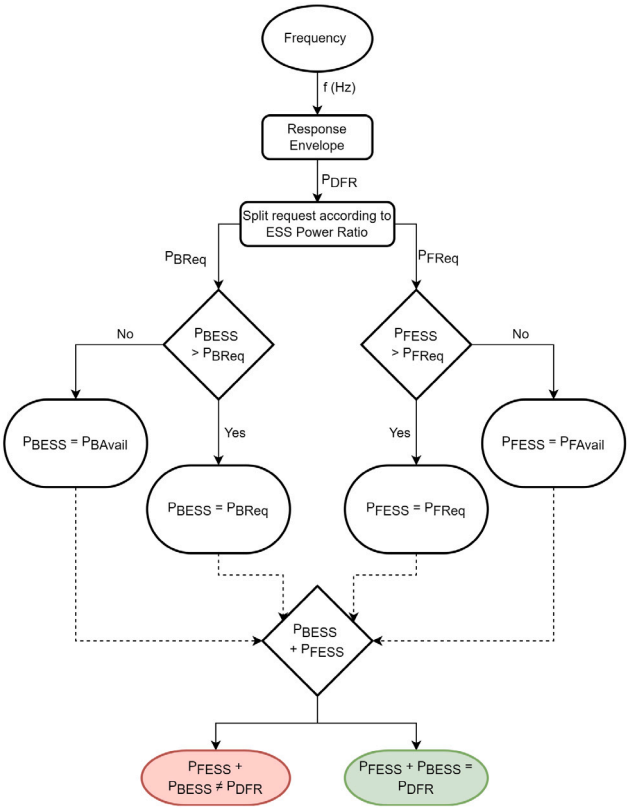


**Fig. 10.** Control diagram and flowchart for Control strategy 5.

**Table 8**
Availability under different FESS configurations for CS-5.

| FESS energy capacity (kWh) | 4C | 8C | 12C |
|---|---|---|---|
| 15 | 96.77% | 96.82% | 96.85% |
| 50 | 96.94% | 96.90% | 96.62% |
| 100 | 96.97% | 95.92% | |
| 150 | 96.80% | | |
| 200 | 96.26% | | |

**Table 9**
BESS degradation under different FESS configurations for CS-5.

| FESS energy capacity (kWh) | 4C | 8C | 12C |
|---|---|---|---|
| 15 | 12.35% | 11.55% | 10.74% |
| 50 | 10.47% | 7.74% | 5.04% |
| 100 | 7.74% | 2.38% | |
| 150 | 5.04% | | |
| 200 | 2.38% | | |

degradation when the FESS configuration is varied, ranging from 2.38% to 12.35% suggesting that in certain scenarios this control strategy actually causes increased degradation in the BESS compared to the BESS-only strategy of CS-1.

This is likely due to the reduction in output causing it to reach SOC limits less often and hence operating for longer, with the FESS not taking enough of a share of the power to provide any benefit. However, in some cases the degradation is significantly reduced extending the life of the BESS and increasing the average availability at the same time.

### 5.2. TCC sensitivity analysis

To further analyse the effectiveness of this control strategy, a TCC sensitivity analysis has been conducted. This was conducted for FESS

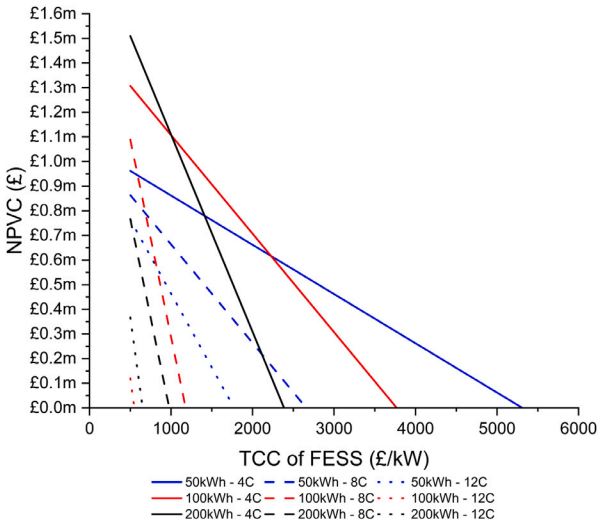


**Fig. 11.** NPVC for varying TCC across different FESS configurations for CS-5.

sizes of 50 kWh, 100 kWh and 200 kWh at varying C-Rates of 4, 8 and 12. The results of this analysis are shown in Fig. 11 showing the NPVC across a range of TCC values designed to show the point at which they cease to profit a positive NPVC (the points at which they reach £0 NPVC), known as the positive NPVC threshold TCC value.

Of the configurations tested, the 200 kWh 4C system shows the highest available NPVC at a TCC of £500/kW, but drops sharply downwards as the TCC is increased. The configurations considered have a TCC profitability threshold between £550/kW and £5,855/kW.

Looking at the leading edge of the graph, the best configurations of FESS for this control strategy are as follows;

- Between £500/kW and £1,000/kW the 200 kWh 4C system is the best performing.
- Between £1,000/kW and £2,225/kW the 100 kWh 4C system is the best performing.
- Above £2,225/kW the 50 kWh 4C system is the best performing.

This suggests that for this control strategy the lower C-Rate configurations are more economically viable in general, with the energy capacity to be installed being dependant on what the current TCC is.

## 6. Control strategy 8

When utilising this control strategy, the ESS responsible for delivering the service is alternated based upon a set duty period. In the initial assessment, this was set to alternate for 30 min of delivery from each ESS in turn. For example, the FESS will be asked to deliver 100% of the requested power for 30 min, followed by the BESS being asked to deliver 100% of the requested power for 30 min. Fig. 12 shows the flowchart for how this strategy is executed.

Fig. 13, shows how the BESS degradation varies according to the duration of time that the FESS is asked to operate with the BESS degrading more the less time the FESS operates for. Even with the FESS operating for 30 min of every hour, this control strategy cannot achieve the same high reductions in BESS degradation as achieved previously with CS-4 and CS-5. However, it still achieves modest reductions in degradation with any time length above 15 min of FESS operation per hour resulting in an overall BESS degradation of less than 10% per year.

### 6.1. C-Rate and energy capacity sensitivity analysis

The main variables of this control strategy are the FESS contribution duration, the FESS energy capacity and the FESS C-Rate. However, this

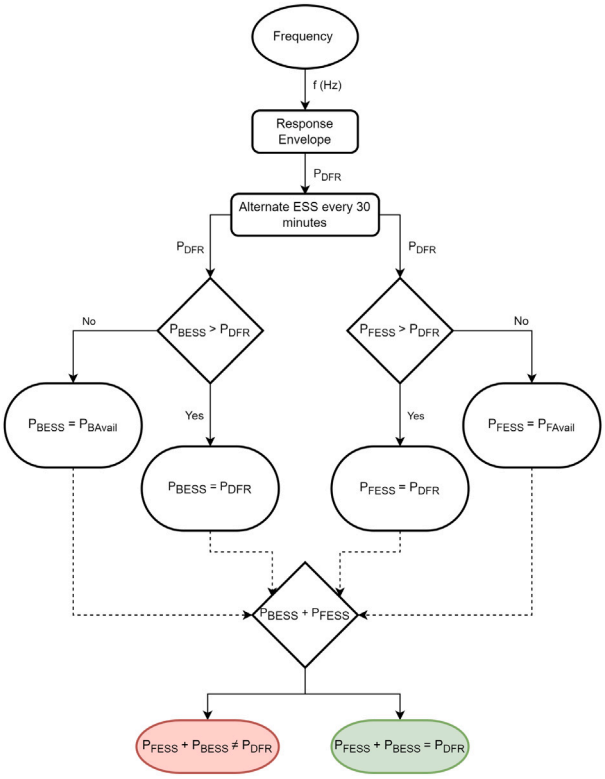


**Fig. 12.** Control diagram and flowchart for Control strategy 8.

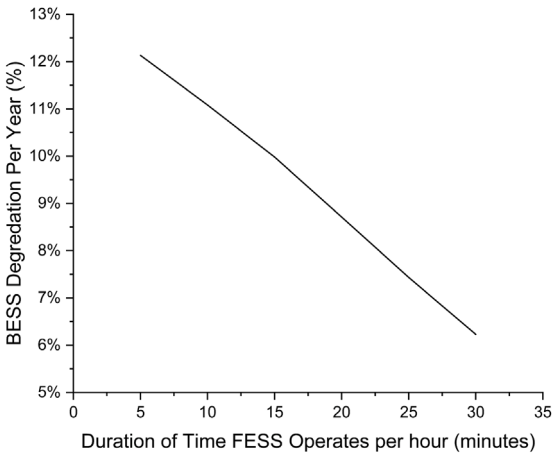


**Fig. 13.** BESS Degradation per year for varying settings of FESS duration of operation per hour for CS-8.

initial assessment consisted of a FESS that provided a maximum of 240 kW of power, meaning it could not provide the required service in the periods that it was active. For this reason, a power based sensitivity analysis was conducted with the power set at 1000 kW and the C-Rate set at 4, 8 and 12C, thus changing the energy capacity of the FESS.

The proportion of an hour that the FESS is active for was also varied between 20 and 30 min with the average availability for these simulations shown in Fig. 14. An initial economic assessment is also shown in Fig. 14, setting the FESS TCC at £500/kW to determine how profitable each combination of C-Rate and FESS contribution duration could be at this cost.

Average availability experiences a steady decline for all 3 variations of C-Rate, with only the 4C system being able to provide an availability above 95% at the lower FESS duration end of the scale. It can be seen

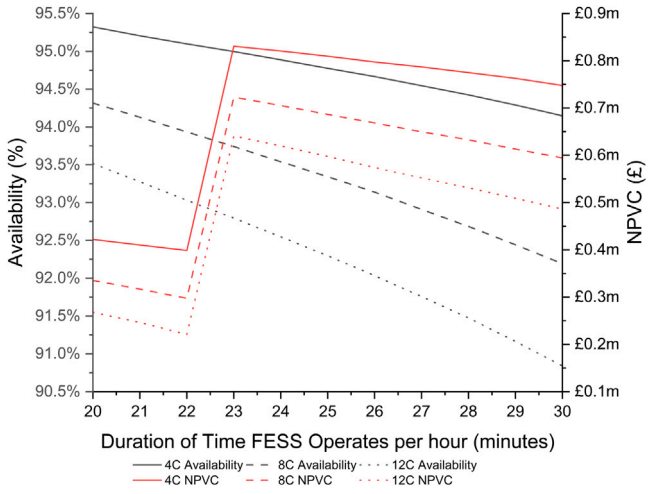


**Fig. 14.** (a) Average Availability and (b) NPVC for different C-Rates of a 1MW FESS, across a range of different FESS operational duration.

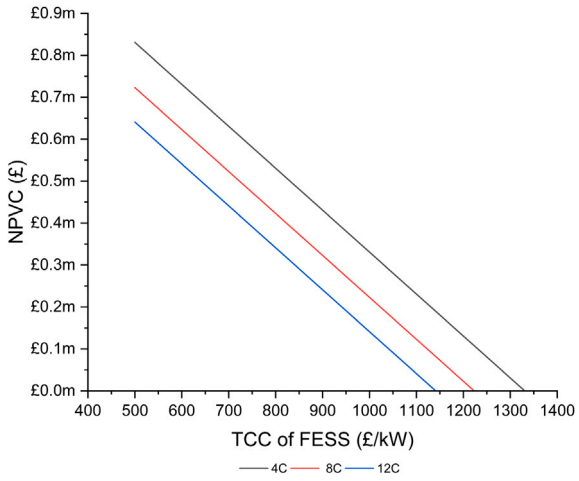


**Fig. 15.** NPVC for varying TCC across different FESS configurations for CS-8.

that the best results at this TCC are achieved with a FESS contribution duration of 23 min, and the overall positive NPVC reduces as the C-Rate of the FESS is increased beyond this point.

In the opposite direction, there is a sharp drop off once the duration is dropped below 23 min, due to the BESS degradation remaining high enough that an additional replacement system is required within the studied time frame. Following this, a threshold TCC for positive NPVC assessment for this level of FESS contribution duration was carried out for the range of C-Rates with the results shown in Fig. 15.

Fig. 15 shows that the positive NPVC threshold TCC for all three systems falls in the £1,141-£1,330/kW range, a position that places it in the middle of the range of existing FESS TCC within current literature. This suggests that all three systems have a chance of introducing a positive NPVC under current costs, with the potential to increase this positive change further as the TCC is reduced.

The 4C system represents the best performing configuration, however the 8C and 12C configurations also perform well enough that systems that fall into the higher C-Rate ranges could be considered under this control strategy.

## 7. Conclusion

A range of different control strategies for hybrid energy storage systems delivering DFR have been presented. It has presented a core methodology around designing and optimising hybrid control strategies to maximise both technical and economical performance. Of the 7 hybrid control strategies discussed, some control strategies did not produce sufficiently promising results to be investigated further due to either high BESS degradation or low average availability.

Despite this, all of the hybrid control strategies provided some degradation reduction in the initial analysis, ranging from a year long BESS degradation of between 2.65% and 12.4% for the hybrid systems compared to a baseline of 13.15%.

The most promising control strategies were investigated further undergoing refinement and economical analysis, showing potential improvements to the NPV of the site across all analysed control schemes. Finally, the TCC at which a FESS will need to be produced to provide an economic benefit has been explored in depth.

The control scheme that produced the best economic performance was Control Scheme 5 with a peak NPVC of £1,509,400. The range of threshold TCC for a positive NPVC was between £550/kW and £5,855/kW. However, the majority of the systems considered were concentrated in the region of a £1,000-£2,500/kW TCC for positive NPVC, which falls in line with common values throughout literature for FESS TCC, and as such shows significant potential for the deployment of FESSs in this area.

Future work should concentrate on further refinement these control strategies, with potential for hybridising other technologies under similar control strategies to assess their suitability.

## CRediT authorship contribution statement

**Andrew J. Hutchinson:** Methodology, Formal analysis, Investigation, Writing – original draft, Visualization. **Daniel T. Gladwin:** Conceptualization, Writing – review & editing, Supervision.

## Declaration of competing interest

The authors declare that they have no known competing financial interests or personal relationships that could have appeared to influence the work reported in this paper.

## Data availability

The authors do not have permission to share data.

## References

[1] National Grid ESO, Firm Frequency Response (FFR), [Online]. Available: https://www.nationalgrideso.com/industry-information/balancing-services/frequency-response-services/firm-frequency-response-ffr?overview.

[2] M.W. Siti, D.H. Tungadio, Y. Sun, N.T. Mbungu, R. Tiako, Optimal frequency deviations control in microgrid interconnected systems, IET Renew. Power Gener. 13 (13) (2019) 2376–2382.

[3] M.W. Siti, D.H. Tungadio, N.T. Nsilulu, B.B. Banza, L. Ngoma, Application of load frequency control method to a multi-microgrid with energy storage system, J. Energy Storage 52 (2022).

[4] National Grid ESO, Dynamic Containment [Online]. Available: https://www.nationalgrideso.com/balancing-services/frequency-response-services/dynamic-containment{#}:{~}:text=DynamicContainment(DC)isdesigned,numerouslossesthaneverbefore.

[5] National Grid ESO, Firm Frequency Response (FFR) post tender reports, 2021, [Online]. Available: https://data.nationalgrideso.com/ancillary-services/firm-frequency-response-post-tender-reports.

[6] National Grid ESO, Historic Frequency Data, 2021, [Online]. Available: https://www.nationalgrideso.com/balancing-services/frequency-response-services/historic-frequency-data.

[7] Y.K. Wu, K.T. Tang, Frequency support by BESS – Review and analysis, Energy Procedia 156 (2019) 187–198.

[8] H. Wyman-Pain, Y. Bian, C. Thomas, F. Li, The economics of different generation technologies for frequency response provision, Appl. Energy 222 (2018) 554–563.

[9] B. Mantar Gundogdu, S. Nejad, D.T. Gladwin, M.P. Foster, D.A. Stone, A battery energy management strategy for U.K. enhanced frequency response and triad avoidance, IEEE Trans. Ind. Electron. 65 (12) (2018) 9509–9517.

[10] B. Gundogdu, D. Gladwin, D. Stone, Battery energy management strategies for UK firm frequency response services and energy arbitrage, J. Eng. 2019 (17) (2019) 4152–4157.
[11] J. Scoltock, D.T. Gladwin, Payment analysis for a BESS providing dynamic frequency response in the irish grid, in: IECON Proceedings (Industrial Electronics Conference), Vol. 2019-Octob, 2019, pp. 2452–2457.
[12] S. Koohi-Fayegh, M.A. Rosen, A review of energy storage types, applications and recent developments, J. Energy Storage 27 (November 2019) (2020) 101047, [Online]. Available: http://dx.doi.org/10.1016/j.est.2019.101047.
[13] B. Xu, A. Oudalov, A. Ulbig, G. Andersson, D.S. Kirschen, Modeling of lithium-ion battery degradation for cell life assessment, IEEE Trans. Smart Grid 9 (2) (2018) 1131–1140.
[14] A.J. Hutchinson, D.T. Gladwin, Modeling and simulation framework for hybrid energy storage systems including degradation mitigation analysis under varying control schemes, in: 2021 International Conference on Electrical, Computer and Energy Technologies, no. December, ICECET, 2022, pp. 1–6.
[15] M.E. Amiryar, K.R. Pullen, A review of flywheel energy storage system technologies and their applications, Appl. Sci. 7 (3) (2017).
[16] X. Dai, K. Wei, X. Zhang, Analysis of the peak load leveling mode of a hybrid power system with flywheel energy storage in oil drilling rig, Energies 12 (4) (2019).
[17] L. Ren, Y. Tang, J. Shi, J. Dou, S. Zhou, T. Jin, Techno-economic evaluation of hybrid energy storage technologies for a solar-wind generation system, Physica C 484 (1037) (2013) 272–275, [Online]. Available: http://dx.doi.org/10.1016/j.physc.2012.02.048.
[18] H. Lee, B.Y. Shin, S. Han, S. Jung, B. Park, G. Jang, Compensation for the power fluctuation of the large scale wind farm using hybrid energy storage applications, IEEE Trans. Appl. Supercond. 22 (3) (2012) 5701904.
[19] J. Li, Q. Yang, P. Yao, Q. Sun, Z. Zhang, M. Zhang, W. Yuan, A novel use of the hybrid energy storage system for primary frequency control in a microgrid, Energy Procedia 103 (April) (2016) 82–87, [Online]. Available: http://dx.doi.org/10.1016/j.egypro.2016.11.253.
[20] L. Barelli, G. Bidini, F. Bonucci, L. Castellini, A. Fratini, F. Gallorini, A. Zuccari, Flywheel hybridization to improve battery life in energy storage systems coupled to RES plants, Energy 173 (2019) 937–950, [Online]. Available: http://dx.doi.org/10.1016/j.energy.2019.02.143.
[21] S. Jalali Kashani, E. Farjah, Applying neural network and genetic algorithm for optimal placement of ultra-capacitors in metro systems, in: 2011 IEEE Electrical Power and Energy Conference, EPEC 2011, IEEE, 2011, pp. 35–40.
[22] B. Olateju, A. Kumar, M. Secanell, A techno-economic assessment of large scale wind-hydrogen production with energy storage in western Canada, Int. J. Hydrogen Energy 41 (21) (2016) 8755–8776, [Online]. Available: http://dx.doi.org/10.1016/j.ijhydene.2016.03.177.
[23] J. Hou, J. Sun, H. Hofmann, Control development and performance evaluation for battery/flywheel hybrid energy storage solutions to mitigate load fluctuations in all-electric ship propulsion systems, Appl. Energy 212 (December 2017) (2018) 919–930, [Online]. Available: http://dx.doi.org/10.1016/j.apenergy.2017.12.098.
[24] X. Wang, D. Yu, S. Le Blond, Z. Zhao, P. Wilson, A novel controller of a battery-supercapacitor hybrid energy storage system for domestic applications, Energy Build. 141 (2017) 167–174.
[25] J. Hou, Z. Song, H.F. Hofmann, J. Sun, Control strategy for battery/flywheel hybrid energy storage in electric shipboard microgrids, IEEE Trans. Ind. Inf. 17 (2) (2021) 1089–1099.
[26] S.D. Sessa, A. Tortella, M. Andriollo, R. Benato, Li-ion battery-flywheel hybrid storage system: Countering battery aging during a grid frequency regulation service, Appl. Sci. (Switzerland) 8 (11) (2018) 1–15.
[27] P. Mouratidis, B. Schubler, S. Rinderknecht, Hybrid energy storage system consisting of a flywheel and a lithium-ion battery for the provision of primary control reserve, in: 8th International Conference on Renewable Energy Research and Applications, no. 03, ICRERA 2019, 2019, pp. 94–99.
[28] A.J. Hutchinson, D.T. Gladwin, Genetic algorithm optimisation of hybrid energy storage system providing dynamic frequency response, in: 2022 IEEE International Symposium on Industrial Electronics, IEEE, 2022.
[29] A.J. Hutchinson, D.T. Gladwin, Verification and analysis of a battery energy storage system model, in: Multi-CDT Conference on Clean Energy and Sustainable Infrastructure, Vol. 00, Elsevier, 2022, pp. 4–9.
[30] T. Feehally, A.J. Forsyth, R. Todd, M.P. Foster, D. Gladwin, D.A. Stone, D. Strickland, Battery energy storage systems for the electricity grid: UK research facilities, in: IET Conference Publications, Vol. 2016, no. CP684, Institution of Engineering and Technology, 2016.
[31] D. Wang, J. Coignard, T. Zeng, C. Zhang, S. Saxena, Quantifying electric vehicle battery degradation from driving vs. vehicle-to-grid services, J. Power Sources 332 (2016) 193–203, [Online]. Available: http://dx.doi.org/10.1016/j.jpowsour.2016.09.116.
[32] J. Wang, J. Purewal, P. Liu, J. Hicks-Garner, S. Soukazian, E. Sherman, A. Sorenson, L. Vu, H. Tataria, M.W. Verbrugge, Degradation of lithium ion batteries employing graphite negatives and nickel-cobalt-manganese oxide + spinel manganese oxide positives: Part 1, aging mechanisms and life estimation, J. Power Sources 269 (2014) 937–948, [Online]. Available: http://dx.doi.org/10.1016/j.jpowsour.2014.07.030.
[33] A.J. Hutchinson, D.T. Gladwin, Genetic algorithm optimisation of hybrid energy storage system providing dynamic frequency response, in: 2022 IEEE 31st International Symposium on Industrial Electronics, ISIE, 2022, pp. 98–103.
[34] A.Z. A.L. Shaqsi, K. Sopian, A. Al-Hinai, Review of energy storage services, applications, limitations, and benefits, Energy Rep. 6 (2020) 288–306, [Online]. Available: http://dx.doi.org/10.1016/j.egyr.2020.07.028.
[35] C.K. Das, O. Bass, G. Kothapalli, T.S. Mahmoud, D. Habibi, Overview of energy storage systems in distribution networks: Placement, sizing, operation, and power quality, Renew. Sustain. Energy Rev. 91 (November 2016) (2018) 1205–1230, [Online]. Available: http://dx.doi.org/10.1016/j.rser.2018.03.068.
[36] F. Goris, E.L. Severson, A review of flywheel energy storage systems for grid application, in: Proceedings: IECON 2018 - 44th Annual Conference of the IEEE Industrial Electronics Society, Vol. 1, IEEE, 2018, pp. 1633–1639.